

# NMR Observation of Rattling Phonons in the Pyrochlore Superconductor $\text{KO}_{\text{S}_2}\text{O}_6$

M. Yoshida, K. Arai, R. Kaido, M. Takigawa, S. Yonezawa, Y. Muraoka, and Z. Hiroi  
*Institute for Solid State Physics, University of Tokyo, Kashiwanoha, Kashiwa, Chiba 277-8581, Japan*

(Dated: December 2, 2024)

We report nuclear magnetic resonance (NMR) studies on the  $\beta$ -pyrochlore oxide superconductor  $\text{KO}_{\text{S}_2}\text{O}_6$ . The nuclear relaxation at the K sites is entirely caused by fluctuations of electric field gradient, which we ascribe to highly anharmonic low frequency oscillation (rattling) of K ions. A phenomenological analysis shows a crossover from overdamped to underdamped behavior of the rattling phonons with decreasing temperature and its sudden sharpening below the superconducting transition temperature  $T_c$ . Absence of the Hebel-Slichter peak in the relaxation rate at the O sites below  $T_c$  also indicates strong electron-phonon coupling.

PACS numbers: 76.60.-k, 74.70.-b, 74.25.Kc

The family of new superconductors  $A\text{Os}_2\text{O}_6$  ( $A = \text{K}, \text{Rb}$ , and  $\text{Cs}$ ) with the pyrochlore structure exhibits many exotic properties. For instance, the superconducting transition temperature  $T_c$  increases substantially with decreasing radius of  $A$  ions ( $T_c = 3.3, 6.3$ , and  $9.6$  K for  $A = \text{Cs}, \text{Rb}$ , and  $\text{K}$ , respectively [1, 2, 3, 4]) and shows non-monotonic pressure dependence [5], in contradiction to what would be expected from the change of density of states alone. Among this family  $\text{KO}_{\text{S}_2}\text{O}_6$  is most anomalous. The electrical resistivity shows strong concave  $T$ -dependence down to  $T_c$  [1, 6], in contrast to the normal  $T^2$ -behavior in Rb and Cs compounds [2, 3, 4]. The  $T$ -linear coefficient of the specific heat  $\gamma = 70$  mJ/K $^2$ mol [7, 8] is highly enhanced over the value obtained from band calculations 10-11 mJ/K $^2$ mol [9, 10].

These anomalies imply large density of low energy excitations, which was originally ascribed to magnetic frustration inherent to the pyrochlore lattice, a network of corner-shared tetrahedra formed by Os atoms. However, the Pauli-like susceptibility [7] excludes local moments on the Os sites. How the frustrated lattice geometry affects properties of itinerant electrons is still an open issue. On the other hand, there is now a growing body of experimental evidence for anharmonic motion of isolated alkaline ions in an oversized cage of Os-O network. The specific heat data show existence of low frequency Einstein modes in addition to the electronic and the Debye contributions for all members of  $A\text{Os}_2\text{O}_6$  [7, 8, 11]. The X-ray results revealed huge atomic displacement parameter for the K sites in  $\text{KO}_{\text{S}_2}\text{O}_6$  [12]. Recently a second phase transition at  $T_p = 7.5$  K was observed for high quality single crystals of  $\text{KO}_{\text{S}_2}\text{O}_6$  [6]. Since the transition is of first order and persists into the normal state in high magnetic fields, it is likely a structural transition associated with the K ion dynamics. Calculation of effective ionic Hamiltonian also indicates instability of K ions in a highly anharmonic potential [15], which might be the origin of various anomalies. Oscillations of isolated ions in a large space have been discussed also in other materials such as clathrate [13] and skutterudite [14] compounds and commonly called “rattling”.

In this Letter, we report results of nuclear magnetic resonance (NMR) experiments on the  $^{39,41}\text{K}$  nuclei (nuclear spin  $I = 3/2$ ) and  $^{17}\text{O}$  nuclei ( $I = 5/2$ ) in  $\text{KO}_{\text{S}_2}\text{O}_6$ . We found that the nuclear relaxation at the K sites is caused entirely by phonons via the electric quadrupole interaction. From a phenomenological analysis we propose that rattling phonons undergo a crossover from underdamped to overdamped behavior with increasing temperature. Strong electron-phonon coupling is indicated by rapid reduction of the damping below  $T_c$ . On the other hand, the relaxation rate at the O sites is sensitive to electronic excitations. Substantial damping of quasiparticles due to rattling phonons near  $T_c$  is indicated by the absence of Hebel-Slichter peak at the O sites. A part of the  $^{39}\text{K}$  NMR results has been reported in the previous publication and interpreted in terms of spin fluctuations [16], which must now be discarded.

Two powder samples of  $\text{KO}_{\text{S}_2}\text{O}_6$  were used in the present experiment. The sample A was prepared by heating a mixture of  $\text{KO}_2$  and  $\text{OsO}_2$  with  $\text{Ag}_2\text{O}$  as an oxidizing agency [1]. The sample B was enriched with  $^{17}\text{O}$  by heating  $\text{KO}_2$  and Os metal in two steps in oxygen atmosphere containing 45 %  $^{17}\text{O}$ . Both samples show identical  $T_c$  of 9.6 K. The nuclear spin-lattice relaxation rate  $1/T_1$  at the  $^{39,41}\text{K}$  sites was measured by the saturation recovery method. Although the K sites have tetrahedral ( $T_d$ ) symmetry, hence should not suffer quadrupole broadening, the  $^{39}\text{K}$  NMR spectra consist of a narrow central line (0.3 kHz HWHM at 8.5T) and a slightly broad satellite line (10 kHz HWHM) probably due to imperfections. Nevertheless the entire spectrum was easily saturated by rf comb-pulses, resulting in single exponential recovery of the spin echo intensity. The  $^{17}\text{O}$  NMR spectra show a quadrupole broadened powder pattern. To determine  $1/T_1$ , the recovery of the spin-echo intensity of the central line as a function of time  $t$  after the inversion pulse was fit to the form [17]  $M_{eq} - M_0\{U \exp(-t/T_1) + V \exp(-6t/T_1) + (1 - U - V) \exp(-15t/T_1)\}$  with  $U$  and  $V$  fixed to the same values at all temperatures.

The temperature ( $T$ ) dependences of  $1/(T_1 T)$  at the  $^{39}\text{K}$  sites is shown in Fig. 1. The inset of Fig. 1(a) displays

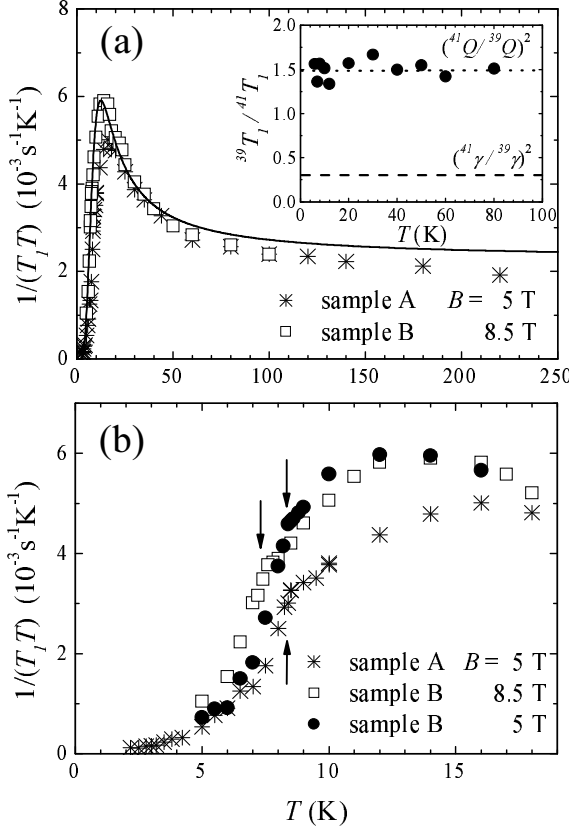


FIG. 1:  $T$ -dependence of  $1/(T_1 T)$  at the  $^{39}\text{K}$  sites for the two samples at different magnetic fields. The data for a wide  $T$ -range are shown in (a). The solid line shows the calculated result of Eq. (5) as described in the text. The inset shows the isotopic ratio of  $1/T_1$ . The dotted (dashed) line indicates the squared ratio of the nuclear quadrupole (magnetic) moments. The data in the low  $T$  region are expanded in (b). The arrows show the superconducting  $T_c$  at the respective fields.

the isotopic ratio  $^{39}T_1/^{41}T_1$  for the sample A. Surprisingly, the isotopic ratio coincides with the squared ratio of the nuclear quadrupole moments  $(^{41}Q/^{39}Q)^2 = 1.48$  rather than the nuclear magnetic moments  $(^{41}\gamma/^{39}\gamma)^2 = 0.30$  in a wide  $T$ -range 6-100 K. Thus the relaxation is entirely caused by fluctuations of electric field gradient (EFG) as opposed to magnetic fluctuations. Their origin cannot be electronic, since all the active electronic states should have dominantly  $s$  character at the K sites and their magnetic coupling to nuclei must be much stronger than the quadrupole coupling. Therefore, it is phonons that cause the nuclear relaxation.

The prominent features of the  $1/(T_1 T)$  data in Fig. 1 are: (1) a peak near 13 K (16 K) for the sample B (A), (2) approximate constant behavior at high temperatures, (3) rapid decrease at low temperatures, (4) a clear kink at the superconducting  $T_c$  and sudden decrease below  $T_c$ . The last point indicates that the behavior of phonons is largely affected by the superconductivity, a direct evidence for strong electron-phonon coupling. The data

from the two samples are slightly different near the peak temperature. Although the reason is not understood clearly, this may arise from different degrees of imperfection or hydration [7].

For nuclei with spin  $3/2$ , the transition probability  $W_q$  between two nuclear levels  $|I_z = m\rangle$  and  $|I_z = m \pm q\rangle$  ( $q = 1$  or  $2$ ) due to quadrupole coupling is given by the correlation function of EFG as [18]

$$W_q = \frac{1}{12} \left( \frac{eQ}{\hbar} \right)^2 \int_{-\infty}^{\infty} \langle [V_{+q}(t), V_{-q}(0)] \rangle e^{iq\omega_L t} dt, \quad (1)$$

where  $\omega_L$  is the nuclear Larmor frequency and  $[A, B]$  stands for  $(AB + BA)/2$ . The irreducible components of the EFG tensor are defined as  $V_{\pm 1} = V_{xz} \pm iV_{yz}$ ,  $V_{\pm 2} = (V_{xx} - V_{yy} \pm 2iV_{xy})/2$ , where  $V_{xy} = \partial^2 V / \partial x \partial y$  etc. is the second derivative of the electrostatic potential at the nucleus. For simplicity we assume spherically symmetric EFG fluctuations. Then  $W_1 = W_2 \equiv W$  and the relaxation rate is given as  $1/T_1 = 2W$ .

In diamagnetic insulators phonons are usually the dominant source of relaxation for quadrupolar nuclei. The ionic motion modulates the EFG,

$$V_{\pm q} = V_{\pm q,0} + \frac{\partial V_{\pm q}}{\partial u} u + \frac{1}{2} \frac{\partial^2 V_{\pm q}}{\partial u^2} u^2 + \dots, \quad (2)$$

where  $u$  is the ionic displacement from the equilibrium position expressed as a linear combination of the phonon creation ( $a^\dagger$ ) and annihilation ( $a$ ) operators. The second term inserted into Eq. (1) leads to the *direct process* [18], which is expressed by the one phonon correlation function or the imaginary part of the susceptibility,

$$W_q \propto k_B T \frac{\text{Im} \chi(q\omega_L)}{q\hbar\omega_L}, \quad (3)$$

provided  $q\hbar\omega_L \ll k_B T$ . For harmonic phonons with infinite life time, the contribution from the direct process is negligible since  $\omega_L$  ( $\sim 10$  MHz) is many orders of magnitude smaller than the typical phonon frequency and the phonon density of states at  $\omega_L$  is practically zero.

On the other hand, the third term in Eq. (2) leads to the *two phonon Raman process*, in which a nuclear transition occurs by absorbing one phonon and emitting another phonon [18]. Usually this is by far the dominant quadrupolar contribution and expressed as  $1/T_1 \propto \int \{\rho(\omega)\}^2 n(\omega) (n(\omega) + 1) |A(\omega)|^2 d\omega$ , where  $n(\omega)$  is the Bose factor,  $\rho(\omega)$  is the phonon density of states, and  $|A(\omega)|$  is the transition matrix element. One can immediately see  $1/T_1 \propto T^2$  at high temperatures where  $n(\omega) \sim T/\omega$ . At low temperatures,  $1/T_1$  decreases monotonically and approaches either to  $T^7$ -dependence for acoustic phonons or activated behavior for optical phonons [18]. Our results in Fig. 1 are, however, in strong contradiction with such behavior.

Since dominance of phonons for nuclear relaxation is extremely rare in metals, we suppose that rattling makes

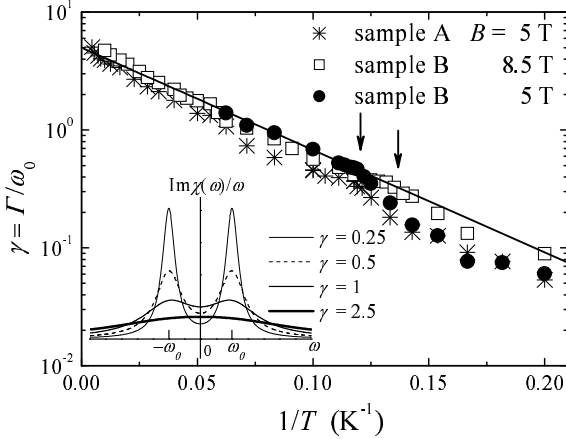


FIG. 2: The normalized damping  $\gamma = \Gamma/\omega_0$  is plotted against  $1/T$ . The arrows correspond to  $T_c$  at 5 T and 8.5 T. The inset shows the phonon line shape  $\text{Im}\chi(\omega)/\omega$  calculated from Eq. (4) for several values of  $\gamma$ .

a special case for  $\text{KO}_{\text{Os}_2}\text{O}_6$ . The distinct features of rattling are its low energy scale and strong anharmonicity, which should lead to damping. We expect that damping-induced broadening of the phonon spectrum peaked at a very low frequency, will bring substantial spectral weight at zero frequency so that the direct process (Eq. 3) becomes important. The peak in  $1/(T_1T)$  is then naturally explained as follows. Let us assume a low frequency Einstein mode at  $\omega_0$ . At low temperatures, the spectrum  $\text{Im}\chi(\omega)/\omega$  is sharp, therefore, the weight at  $\omega_L \approx 0$  should be small. As the spectral width increases with increasing temperature, the weight at  $\omega = 0$  will grow and take a maximum when the width becomes comparable to  $\omega_0$ . Further broadening, however, will spread the spectrum over higher frequencies and reduce the weight at  $\omega = 0$ . (See the inset of Fig. 2.) Thus the peak in  $1/(T_1T)$  can be reproduced if the rattling undergoes a crossover from underdamped to overdamped behavior with increasing temperature. The contribution from the Raman process should be also influenced by damping [19]. However, we could not reproduce the peak in  $1/(T_1T)$  by the Raman process without fine tuning the  $T$ -dependence of the damping. We consider that the Raman process is unimportant. The details will be discussed elsewhere [20].

In order to quantify the above picture, we employ a suitable phenomenological model describing strongly damped oscillators. A commonly used expression is the damped harmonic oscillator model,  $\text{Im}\chi(\omega)/\omega = \Gamma/(\{\omega_0^2 - \omega^2\}^2 + \Gamma^2\omega^2)$ , which leads to  $1/(T_1T) \propto \Gamma/\omega_0^4$  by taking the limit  $\omega_L \rightarrow 0$  in Eq. (3). However, this model is unable to reproduce the observed peak for any monotonic change of the damping  $\Gamma$ . In the damped harmonic oscillator model, only the friction or the momentum relaxation is considered as the sources of damping. It was argued, however, that in the collision dominated regime one must also consider the jump of the spatial coordinate

or the amplitude relaxation [21, 22]. One then obtains the van Vleck-Weisskopf formula [23], which should be suitable for strongly damped anharmonic phonons,

$$\frac{\text{Im}\chi(\omega)}{\omega} = \frac{\Gamma/\omega_0}{(\omega + \omega_0)^2 + \Gamma^2} + \frac{\Gamma/\omega_0}{(\omega - \omega_0)^2 + \Gamma^2}. \quad (4)$$

From Eqs. (4) and (3) we obtain in the limit  $\omega_L \rightarrow 0$ ,

$$\frac{1}{T_1T} \propto \frac{1}{\omega_0^2} \frac{\gamma}{1 + \gamma^2}, \quad (5)$$

where  $\gamma = \Gamma/\omega_0$ . For a fixed value of  $\omega_0$ , this formula has a maximum at  $\gamma = 1$ , which corresponds to the observed peak. By identifying the  $T$ -ranges below or above the peak temperature with the underdamped ( $\gamma \leq 1$ ) or the overdamped ( $\gamma \geq 1$ ) regions and assuming that  $\omega_0$  is constant, we extracted the  $T$ -dependence of  $\gamma$  from the experimental data of  $1/(T_1T)$  as shown in Fig. 2. The result above  $T_c$  is well represented by an activation law  $\gamma = \gamma_0 \exp(-E/k_B T)$  with  $\gamma_0 = 5$  and  $E = 20$  K (the solid line). Thus our analysis predicts extremely overdamped behavior at high temperatures. Note that the phonon frequency  $\omega_0$  cannot be determined from our analysis. The solid line in Fig. 1 shows the  $T$ -dependence of  $1/(T_1T)$  calculated from Eq. (5) and this activation law. A possible interpretation of the activated behavior is that  $\Gamma$  represents the hopping frequency of the K ions among different metastable positions in highly anharmonic potential [15] and the activation energy corresponds to the potential barrier between them.

We have also measured the relaxation rate for  $^{85}\text{Rb}$  and  $^{87}\text{Rb}$  nuclei in  $\text{RbOs}_2\text{O}_6$  and separated the phononic and magnetic contributions [20]. The phonon contribution to  $1/(T_1T)$  in  $\text{RbOs}_2\text{O}_6$  does not show a peak, indicating underdamped behavior in the whole  $T$ -range below the room temperature. The  $T$ -dependence of  $\gamma$  in  $\text{RbOs}_2\text{O}_6$  obtained from similar analysis is also compatible with an activation law with  $E = 12 - 20$  K, although the accuracy is limited.

A remarkable feature of the results in Fig. 2 is the sudden reduction of  $\gamma$  below the superconducting  $T_c$ . This indicates that the damping of rattling phonons near  $T_c$  is primarily caused by electron-phonon interaction and the phonon life time is enhanced by opening of the superconducting gap. Therefore,  $\omega_0$  should be smaller than  $2\Delta \sim 50$  K [7], where  $\Delta$  is the superconducting gap.

We now discuss the results at the O sites. Figure 3 shows the  $T$ -dependence of  $1/(T_1T)$  at the O sites at the fields of 2 T and 8.5 T. Unlike the result for the K sites,  $1/(T_1T)$  is only weakly  $T$ -dependent above  $T_c$ , approximately consistent with the Korringa relation. Thus the spin dynamics of conduction electrons are probed at the O sites. This is consistent with the Os-5d( $t_{2g}$ ) and O-2p hybridized nature of the conduction band [10, 15]. However, the weak  $T$ -dependence of  $1/(T_1T)$  in the normal state is still anomalous and suggests development of mod-

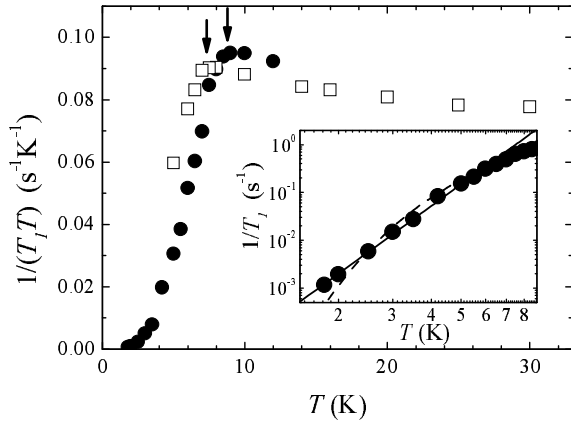


FIG. 3:  $T$ -dependence of  $1/(T_1 T)$  at the  $^{17}\text{O}$  sites at 2 T (solid circles) and 8.5 T (open squares). The arrows indicate  $T_c$  at the respective fields. The inset shows the fitting to a power-law  $1/T_1 \propto T^\alpha$  with  $\alpha = 4.7$  (solid line) and an activation law  $1/T_1 \propto \exp(-\Delta/T)$  with  $\Delta = 17$  K (dashed line) for the data at 2 T below  $T_c$ .

est spin correlation. Below  $T_c$ ,  $1/(T_1 T)$  decreases monotonically. This contradicts with the behavior in weak coupling BCS superconductors with an isotropic gap, where  $1/(T_1 T)$  shows a peak near  $0.9T_c$  (the Hebel-Slichter peak) [24]. At lower temperatures,  $T$ -dependence of  $1/T_1$  can be fit either by a power law  $1/T_1 \propto T^\alpha$  with  $\alpha \sim 5$  or by an activation law  $1/T_1 \propto \exp(-\Delta/T)$  with  $\Delta = 17$  K. Since the upper critical field  $H_{c2}$  is about 30 T at  $T = 0$  [25, 26], pair breaking effects of magnetic field should be negligible at 2 T.

The behavior at low temperatures rules out highly anisotropic gap structure such as line nodes, which leads to  $T^3$  dependence of  $1/T_1$ . This is consistent with the field independent thermal conductivity showing an isotropic gap [27]. Absence of the Hebel-Slichter peak has been often considered as evidence for an anisotropic gap. Since strong anisotropy is ruled out in the present case, it appears more likely due to inelastic scattering of quasiparticles by phonons, which broadens the superconducting density of states as was proposed for the case of  $\text{TiMo}_6\text{Se}_{7.5}$  [28]. This has been also predicted by numerical calculations based on the Eliashberg theory [29, 30]. The calculation by Akis *et al.* [30], for example, shows that the Hebel-Slichter peak disappears when  $k_B T_c / \hbar \omega_{ln}$  is larger than  $0.2 \sim 0.3$ , where  $\omega_{ln}$  is the Allen-Dynes parameter representing the typical phonon frequency. This is compatible with our previous conclusion that the frequency of the rattling phonon is smaller than  $2\Delta \sim 5k_B T_c$ . Whether the rattling works as a pairing mechanism or acts as a pair breaker is still an open question.

In conclusion, our analysis of the  $1/(T_1 T)$  data at the K sites indicates a crossover of rattling from the low  $T$

underdamped to high  $T$  overdamped behavior near 13 - 16 K. The rapid decrease of  $1/(T_1 T)$  at the K sites below  $T_c$  indicates strong electron-phonon coupling and enhancement of the lifetime of rattling phonons. Hence its frequency must be smaller than  $2\Delta$ . The results at the O sites rule out strongly anisotropic gap. The absence of the Hebel-Slichter peak at the O sites is also compatible with strong electron-phonon coupling.

We thank T. Kato, Y. Takada, H. Maebashi K. Ishida, H. Harima, H. Fukuyama, Y. Matsuda, and S. Tajima for valuable discussions. This work was supported by a Grant-in-Aid for Scientific Research on Priority Areas (No. 16076204 “Invention of Anomalous Quantum Materials”) from the MEXT Japan.

---

- [1] S. Yonezawa *et al.*, *J. Phys.: Condens. Matter* **16**, L9 (2004).
- [2] S. Yonezawa *et al.*, *J. Phys. Soc. Jpn.* **73**, 819 (2004).
- [3] M. Brühwiler *et al.*, *Phys. Rev. B* **70**, 020503(R) (2004).
- [4] S. Yonezawa, Y. Muraoka, and Z. Hiroi, *J. Phys. Soc. Jpn.* **73**, 1655 (2004).
- [5] T. Muramatsu *et al.*, *Phys. Rev. Lett.* **95**, 167004 (2005).
- [6] Z. Hiroi *et al.*, *J. Phys. Soc. Jpn.* **74**, 1682 (2005).
- [7] Z. Hiroi, S. Yonezawa, Y. Nagao, and J. Yamaura, unpublished.
- [8] M. Brühwiler *et al.*, *Phys. Rev. B* **73**, 094518 (2006).
- [9] J. Kuneš, T. Jeong, and W. E. Pickett, *Phys. Rev. B* **70**, 174510 (2004).
- [10] R. Saniz *et al.*, *Phys. Rev. B* **70**, 100505(R) (2004).
- [11] Z. Hiroi *et al.*, *J. Phys. Soc. Jpn.* **74**, 1255 (2005).
- [12] J. Yamaura *et al.*, *Solid State Chem.* **179**, 336 (2006).
- [13] V. Keppens *et al.*, *Nature* **395**, 876 (1998).
- [14] S. Paschen *et al.*, *Phys. Rev. B* **64**, 214404 (2001).
- [15] J. Kuneš and W. E. Pickett, *Phys. Rev. B* **74**, 094302 (2006).
- [16] K. Arai *et al.*, *Physica* **B359-361**, 488 (2005).
- [17] A. Narath, *Phys. Rev.* **162**, 320 (1967).
- [18] A. Abragam, *The principles of Nuclear Magnetism* (Oxford University Press, Oxford, 1961).
- [19] M. Rubinstein and H. A. Resing, *Phys. Rev. B* **13**, 959 (1976).
- [20] M. Yoshida *et al.*, unpublished.
- [21] B. D. Silverman, *Phys. Rev. B* **9**, 203 (1974).
- [22] Y. Takagi, *J. Phys. Soc. Jpn.* **47**, 567 (1979).
- [23] J. H. van Vleck and V. F. Weisskopf, *Rev. Mod. Phys.* **17**, 227 (1945).
- [24] L. C. Hebel and C. P. Slichter, *Phys. Rev.* **113**, 1504 (1959).
- [25] E. Ohmichi *et al.*, *J. Phys. Soc. Jpn.* **75**, 045002 (2006).
- [26] T. Shibauchi *et al.*, cond-mat/0603309.
- [27] Y. Kasahara *et al.*, *Phys. Rev. Lett.* **96**, 247004 (2006).
- [28] Y. Kitaoka *et al.*, *Physica* **C192** 272 (1992).
- [29] P. B. Allen and D. Rainer, *Nature* **349**, 396 (1991).
- [30] R. Akis, C. Jiang, and J. P. Carbotte, *Physica* **C176**, 485 (1991).